© 2023 Association for Computing Machinery. This is the author's version of the work. It is posted here for your personal use. Not for redistribution. The definitive Version of Record was published in UIST '22: Proceedings of the 35th Annual ACM Symposium on User Interface Software and Technology. October 2022. Article No. 60. Pages 1–11 https://doi.org/10.1145/3526113.3545675

TipTrap: A Co-located Direct Manipulation Technique for Acoustically Levitated Content.

Eimontas Jankauskis
e.jankauskis@ucl.ac.uk
University College London
London, UK

Sonia Elizondo
Universidad Publica de Navarra
Pamplona, Spain
sonia.elizondo@unavarra.es

Roberto Montano Murillo
University College London / Ultraleap
London / Bristol, UK
roberto.montano@ultraleap.com

Asier Marzo
Universidad Publica de Navarra
Pamplona, Spain
asier.marzo@unavarra.es

Diego Martinez
University College London
London, UK
d.plasencia@ucl.ac.uk

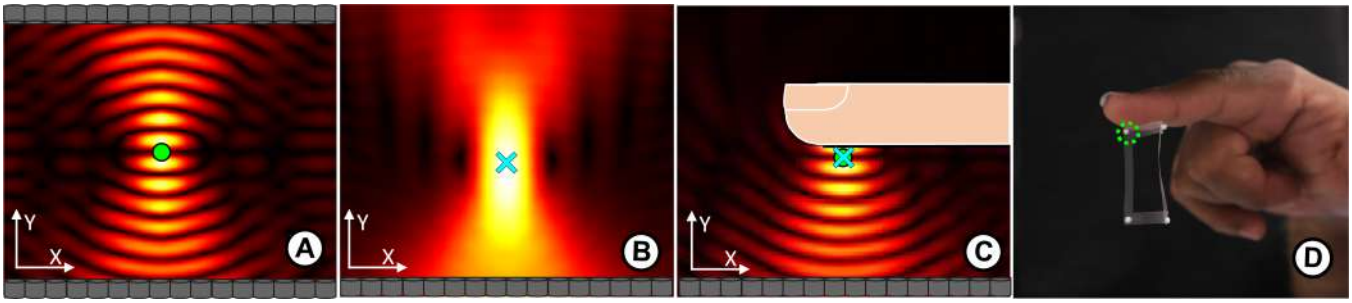

Figure 1: TipTrap leverages sound reflections on the fingertip for co-located direct manipulation of levitated content. a) A conventional levitation trap in open space holding a particle. b) A focal point in open space cannot levitate a particle. c) A focal point reflected off the user's skin creates an *opportunistic trap (OT)*, which can hold particles under the fingertip. d) TipTrap creates *OT*s under the users' tips to enable co-located direct manipulation of levitated content.

ABSTRACT

Acoustic levitation has emerged as a promising approach for mid-air displays, by using multiple levitated particles as 3D voxels, cloth and thread props, or high-speed tracer particles, under the promise of creating 3D displays that users can see, hear and feel with their bare eyes, ears and hands. However, interaction with this mid-air content always occurred at a distance, since external objects in the display volume (e.g. user's hands) can disturb the acoustic fields and make the particles fall. This paper proposes TipTrap, a co-located direct manipulation technique for acoustically levitated particles. TipTrap leverages the reflection of ultrasound on the users' skin and employs a closed-loop system to create functional acoustic traps 2.1 mm below the fingertips, and addresses its 3 basic stages: selection, manipulation and deselection. We use Finite-Differences Time Domain (FDTD) simulations to explain the principles enabling TipTrap, and explore how finger reflections and user strategies influence the quality of the traps (e.g. approaching direction, orientation and tracking errors), and use these results to design our technique. We then implement the technique, characterizing its performance with a robotic hand setup and finish with an exploration of the ability of TipTrap to manipulate different types of levitated content.

Permission to make digital or hard copies of all or part of this work for personal or classroom use is granted without fee provided that copies are not made or distributed for profit or commercial advantage and that copies bear this notice and the full citation on the first page. Copyrights for components of this work owned by others than ACM must be honored. Abstracting with credit is permitted. To copy otherwise, or republish, to post on servers or to redistribute to lists, requires prior specific permission and/or a fee. Request permissions from permissions@acm.org.
Conference'17, July 2017, Washington, DC, USA
© 2023 Association for Computing Machinery.
ACM ISBN 978-x-xxxx-xxxx-x/YY/MM…$15.00
https://doi.org/10.1145/nnnnnnn.nnnnnnn

CCS CONCEPTS

• **Human-centered computing** → *Gestural input*; • **Hardware** → *Emerging interfaces.*

KEYWORDS

co-located direct manipulation, acoustic levitation, interaction techniques, spatial interaction

ACM Reference Format:
Eimontas Jankauskis, Sonia Elizondo, Roberto Montano Murillo, Asier Marzo, and Diego Martinez. 2023. TipTrap: A Co-located Direct Manipulation Technique for Acoustically Levitated Content.. In *Proceedings of ACM Conference (Conference'17).* ACM, New York, NY, USA, 11 pages. https://doi.org/10.1145/nnnnnnn.nnnnnnn

1 INTRODUCTION

Acoustic levitation is emerging as an approach to create interactive mid-air displays, with quick advances in the last few years. Graphics created by the levitating particles provide the users with all the depth clues of true-3D graphics, since the particles act as voxels that physically exist in space. Such content can be observed by

multiple viewers, from different points of view and without any barriers between the users and the levitated content [18].

The graphics rendered by acoustic levitation can take several forms: content made of various independent levitated particles, acting as sparse 3D voxels [28, 34]; particles attached to fabric props or threads [11, 31]; or high-speed tracer particles that produce persistence-of-vision (POV) shapes [14]. These techniques operate in real time and can be combined with tactile and auditory feedback, advancing towards a display that users can see, hear and feel with their bare eyes, ears and hands [18, 40].

This has attracted the interest of the HCI community, which has started to explore applications [31, 34, 35, 37] and interaction techniques, such as Point-and-Shake [13] for particle selection or LeviCursor [3] for manipulation. However, such interaction techniques only allow interaction at a distance. That is, while the users will be able to see the 3D levitated content in front of them without any barriers, they will not be able to reach in and directly interact with the content (i.e. input and output spaces do not overlap [19]). To date, only ray-based selection and manipulation at a distance had been used, as hands that are close to the content can disrupt the acoustic field, causing levitated content to fall as ultrasound reflects off the users' hands.

Rather than avoiding ultrasound reflections off the users' hands, our TipTrap technique exploits them, as summarized in Figure 1. Figure 1.A shows how the acoustic pressure distributes around a conventional levitation trap created by a top-bottom levitation setup in the absence of external objects. Figure 1.B shows a focal point generated just from the bottom array, as typically used in haptics, but unable to levitate particles. However, we note that when this focal point is reflected off the users' skin (see Figure 1.C), the pressure distribution appearing $\sim$ 2.1 mm below the fingertip is very similar to that of a conventional levitation trap (see similarities with Figure 1.A). By tracking the users' fingertips in a closed loop and focusing the position of the traps under them, TipTrap allows selection and manipulation of particles in near-contact proximity to the fingertips ($\sim$ 2.1 mm), enabling co-located, direct manipulation [19] of different types of levitated content (e.g., Figure 1.D).

As a core contribution, we present the concept of *Opportunistic Traps (OTs)* which are acoustic traps intentionally created near a reflective and locally flat object, and exploit *OTs* to create TipTrap, the first co-located direct manipulation technique for levitated content.

2 RELATED WORK

We first review related literature in the field of 3D displays, focusing on how no existing approach allows uninstrumented users to see the 3D content and interact with it in a direct co-located fashion. We then analyze interaction techniques for levitation displays, highlighting how no existing technique allows such co-located direct interactions.

2.1 Mid-air 3D displays

There are several categories of 3D displays which allow uninstrumented users to directly see the 3D content from any point around the display. While seeing content is possible, no approach allows bare-handed, direct, co-located interaction with such 3D content. Holographic and lenslet displays [49] rely on a two-dimensional (2D) display modulator, requiring direct line of sight from the observer's eyes to the content and the display surface, which limits their viewing angles. Besides, real objects such as fingers occluding the modulator will always appear in front of the content, causing incorrect occlusions and eye fatigue [47].

Light converging optical elements such as optical combiners, concave mirrors and Fresnel lenses can create mid-air images behind the optical element [16, 17, 22, 24, 41], avoiding occlusion and eye fatigue [24]. However, the optical combiners between the user and the content hinder reachability and co-located interaction. Particulate displays use particles floating in air, such as water drops [5, 9], fog [25, 42, 44, 51] or dust [39], allowing reachability, but they are limited to 2D projections from a limited number of viewpoints.

Swept volume displays create 3D geometries by quickly moving a flat surface that emits [46] or reflects [20] light from points within the 3D space. Solid state approaches [10, 21, 50] stack display panels such as LCDs to render 3D content. In these approaches, 3D depth and parallax can be provided and content is viewable around the display [7]. However, content is not directly reachable and interaction is limited to non-collocated interactions [4].

Free Space Displays generate 3D geometries without any physical barriers between the user and the content, the content is visible from any point around the display. These displays use laser induced plasma voxels [45] or particles levitated via electrophoresis [6], magnetophoresis [23], optophoresis [48] or acoustophoresis [18, 28]. Among these, ZeroN stands as the only alternative allowing co-located, direct manipulation of the 3D content, but it is limited to a single element of fixed geometry and material (i.e. a metal sphere). In all the other cases, objects inserted inside the display to manipulate the content will either get damaged by the plasma or interrupt the levitation mechanism.

2.2 Interactions with levitated particles

We focus our exploration in acoustic setups using two opposing Phased Arrays of Transducers (top-bottom PATs), as this is the most common setup used for display purposes. We highlight the different levitated content that can be created, as well as existing limitations to interactions with such content.

PAT setups first enabled limited control of single particles [35], particles attached to threads [36], or sets of particles moved as a group [34]. Full 3D control of particles was enabled by the holographic method [29], enabling free 3D control of single particles in any levitator arrangement. This was later extended to allow independent control of up to 27 particles [28] enabling the creation of simple 3D shapes with the particles acting as sparse voxels. These 3D shapes can be combined with external cloth props, either as fixed parts of the background [12], or attached to the levitating particles to create mid-air projection screens [31]. Fast computation of levitation traps allowed the creation of continuous (as opposed to sparse) levitated 3D content by using either a single [14, 18, 38] or multiple [40] high-speed tracer particles.

Point and Shake [13] provides a selection technique for levitated particles based in a ray-casting technique, shaking particles for disambiguation. LeviCursor [3] explores the use of a levitated particle as a 3D cursor, also using a remote ray casting technique.

These distant interactions techniques have been adopted by related applications, such as LeviLoop [32] or the shooting game in [37].

Few exceptions exist allowing closer interactions. GauntLev [26] allowed levitation between the user fingers by attaching wearable PATs to each finger but the particles always stayed between the fingers with limited display capabilities. Hirayama et al. [18] demonstrated tactile feedback in the users' hands with simultaneous 3D content, but the hands needed to remain at least 20 mm away from the content and never on top or below them, and interaction opportunities were not explored. The racket and ball game in [37] overcame this by using a tool to almost touch the levitated particle, made of a very thin wire that produced negligible ultrasound reflections.

Finally, only a few approaches have allowed external objects inside the levitator. SoundBender [33] used self-bending beams to minimize ultrasound reflections to enable levitation or haptics above static passive props placed on top of the emitter array. Single sided arrays and flat reflectors have been used to create levitation traps above the reflector (i.e. hovering) [2], but only for static and flat reflectors. None of these approaches leverage reflections on dynamic objects or body parts for direct, co-located interaction.

3 CHARACTERIZING OPPORTUNISTIC TRAPS

TipTrap relies on the exploitation of *Opportunistic Traps* (*OTs*) created under the fingertips. We define *OTs* as acoustic traps that are intentionally created by a system in the proximity of acoustically reflective and locally flat object (e.g., the fingertip), by reflecting focused ultrasound off such surface (see Figure 1.B and C).

This section focuses on the use of a fingertip to create *OTs*. More specifically, we provide a characterisation of the properties of an *OT* created by an average-size finger modelled as a capsule-cylinder of 15mm diameter and a top-bottom PAT setup, which is the most common arrangement used for acoustic levitation displays.

For this top-bottom setup, *OTs* can be created from reflecting ultrasound off the users' finger, either by using a focal point or a levitation trap. In the latter case, the ultrasound coming from the top array is occluded by the finger so both approaches (trap or focal point) behave in a very similar way, resulting in an *OT* located $\lambda/4 =\sim 2.1$ mm below the fingertip. Please note that the *OT* will always appear at that position (~ 2.1 mm below the fingertip), even if ultrasound is targeted slightly above/below the skin and independently of the type of field (i.e., focal point or levitation trap).

We recommend the use of levitation traps, instead of focal points. This is useful for when the fingertip is not placed at the right location due to tracking errors or delays. In this case, the focal point approach would not create a trap at all and the particle would be ejected or fall. In contrast, if a levitation trap is used, content can be levitated in the absence of the finger, and trapped under the fingertip with an *OT* when the correct interaction is detected.

Given the high acoustic impedance of human skin or nails compared to air, *OTs* can be created either below or above the finger (i.e. above the nail) with very similar behaviour. This can provide mechanisms to avoid the finger from occluding the particle by levitating the particle above the nail, when the hand is below eye level,

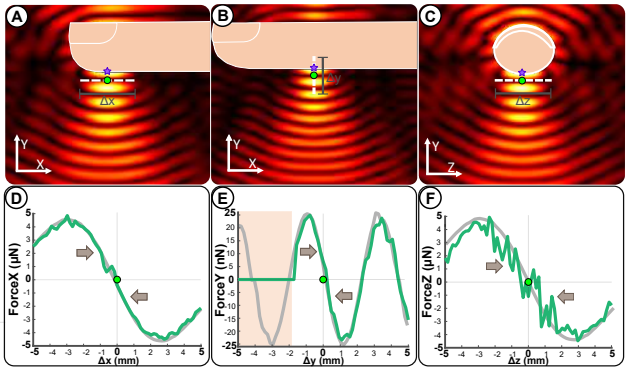

Figure 2: Analysis of forces around an Opportunistic Trap created at the user's fingertip, along: X (left), Y (centre), and Z (right). The top row shows the pressure distribution around the trap; and the bottom row shows forces (green) along the axes compared to a traditional levitation trap, with no other objects present (grey).

but we constraint our analysis to *OTs* bellow the tip for simplicity in this paper.

To characterize the behaviour of *OTs*, we use a numerical simulation using Finite-difference time-domain (FDTD) to assess the viability of *OTs* for stable levitation. More specifically, we compare the trapping forces created by an *OT* under the finger with those created by a conventional levitation trap, showing very similar trapping characteristics (Figure 2).

3.1 Numerical simulation method

We used Finite-difference time-domain method (FDTD) to simulate the acoustic field, forces and trapping stiffness of the *OTs*, taking into account the reflections caused by the users' finger. We cannot use the typical piston model employed to calculate the acoustic field [27] since it operates under the assumption of an empty volume and cannot simulate ultrasound reflections off any objects inside it.

In FDTD, the simulation space (domain), is divided into cells that contain the value for the pressure and velocities. In each iteration, the new domain state is calculated from the previous one, with each cell being updated using the values of its surrounding cells.

We use an implementation adapted from [1], applying the methods on sections 3.1 and 3.2. Our working frequency is 40 kHz, the simulation space is 16 cm along each dimension, which we divide in 1024 cells for a cell size of 0.0194 wavelengths (the minimum recommended is 0.1). The timestep was 0.17 μs and the damping on the system was set to $0.999Pa^{-1}$.

We allowed a ramp-up period for the waves to propagate and reflect 8 times from side to side of the domain, so that its state became stable. We then computed peak amplitudes and phases at each cell, by taking into account 2 periods of the wave to convert the time domain amplitude results into frequency domain results (i.e., amplitude and phase). Thus, instead of looking at the amplitude value at each timestep, we use the 40KHz component of our frequency results to determine the amplitude and phase at each cell in space (i.e. the complex field).

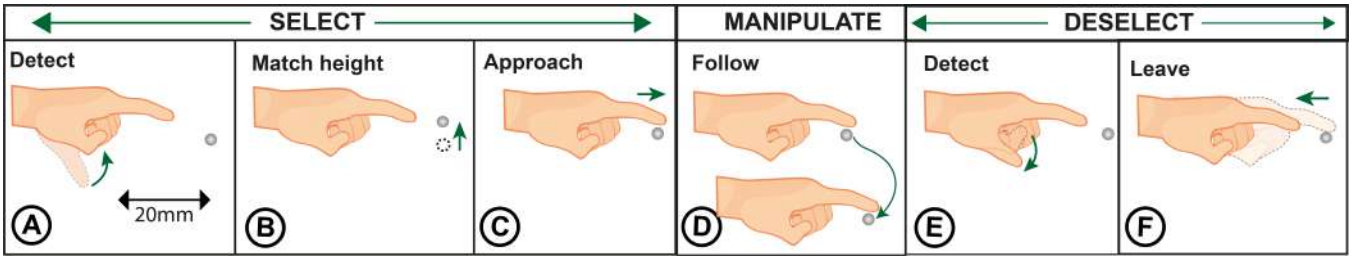

Figure 3: TipTrap has three main stages: During Selection, the user performs a command (a). When the fingertip is closer than 20 mm from the particle, the system adjust the height to transition into the OT (b) while the user brings the fingertip close to the particle (c); During Manipulation, a closed-loop system allows the OT to be refocused under the current location of the fingertip (d); Deselection is triggered by another command (e) and the particle remains at its position as it is released (f).

Having the amplitude and phase is not enough for determining the forces acting on the particles. We used them to compute the Gork'ov potential [15] which represents the potential acting on the particles that are inside the acoustic field. The negative gradient of this potential provides the forces exerted on a particle. We also use the Laplacian of the potential (i.e., the second derivative) to report the stiffness of the trap. The stiffness represents how converging are the forces around a point and they can be used to measure the quality of the acoustic traps [29].

3.2 Viability of Opportunistic Traps

In order to assess the viability of *OTs*, we analysed how forces distribute along each of the axes for an *OT*, placed 2.1 mm below the user's fingertip. For the remaining of the paper, we will use the position where the *OT* is created as a reference (i.e., zero distance in our plots), with the *OT* being placed at 15 mm from the tip and 2.1 mm below it (see Figure 2.A). The location of the *OT* will also be visually denoted as a green circle in all our plots.

The pressure distribution (i.e. amplitude field) around the *OT* is shown in the top row of Figure 2, showing great similarity to those generated by a conventional levitation trap (i.e. see Figure 1.A).

The second row of Figure 2 shows the trapping forces experienced by a particle as it gets displaced along each axis of the *OT*. Such forces are compared against the equivalent trapping forces produced around a conventional levitation trap placed at the same location, but in the absence of a finger (i.e., grey line in Figure 2).

These force distributions show strong converging forces around the OT along all 3 axis. For example, if a trapped particle moves to the right (positive X), it will experience a negative force along the X axis, pushing it back to the centre of the trap. As such, the presence of these restorative forces along all axes illustrate the feasibility of *OTs* to operate as functional levitation traps.

The peak forces of the *OT* in our top-bottom setup are approximately 4.9 μN along the X-axis, 24μN along Y, and 5μN along Z. These ratios are coherent with those produced by a typical levitation trap [29], where the traversal trapping force (Y in our case) is approximately 8 times larger than the lateral forces (X and Z in our case). This indicates that *OTs* behave very similarly to a conventional levitation trap, once a particle is placed inside it.

4 TIPTRAP: TECHNIQUE OVERVIEW

The previous section showed the capability of *OTs* to act as viable levitation traps, that is, to keep particles trapped in an *OT* with converging forces along all axes.

Given the variations in the definition of a *Direct* manipulation technique, we define *TipTrap* as a direct, co-located technique, with levitated content following the motion of the users' hands and overlap of the input and output spaces. *TipTrap* also address the 3 steps in manipulation [8]: selection, manipulation and deselection.

We used FDTD simulations to identify feasible approaches to implement each step (i.e., selection, manipulation and deselection), as well as to derive key parameters influencing their performance. This analytical exploration led to the design of the TipTrap technique, which we summarize below and in Figure 3. The justification for this design is based in our FDTD simulations and will be detailed in the following subsections.

- **Selection:** The first stage of TipTrap is the *Selection* stage, summarized in Figures 3.A, B and C. We assume a generic 'select' command is used to trigger the technique (e.g., flexing the thumb, as in Figure 3.A). Once the fingertip enters within the 20 mm range where it can affect the particle trap [18], the particle is automatically adjusted to allow an optimum transition to an *OT* below the fingertip (Figure 3.B). More specifically, the particle aligns to the finger lateral displacements (Z) and retains a height < 2.1 mm below the fingertip (Y). This stage finishes when the user slides in the finger, placing the particle at the target location (*OT*) under the fingertip (see Figure 3.C).
- **Manipulation:** This second stage supports free movement (i.e., *Manipulation*) of the particle (Figure 3.D). Once the particle has been moved into the OT, the position of the acoustic trap is locked on to the fingertip. This maintains the *OT* under the fingertip; thereby, while the user moves their fingertip around the interaction volume, the particle moves along with it.
- **Release** The *Release* stage is the final stage of the technique. Similarly to the *Selection* stage, this stage begins when the system recognises an arbitrary gesture (Figure 3.E) such as unbending the thumb. The acoustic trap then stops following the finger and the user can remove their hand from the levitation space (Figure 3.F).

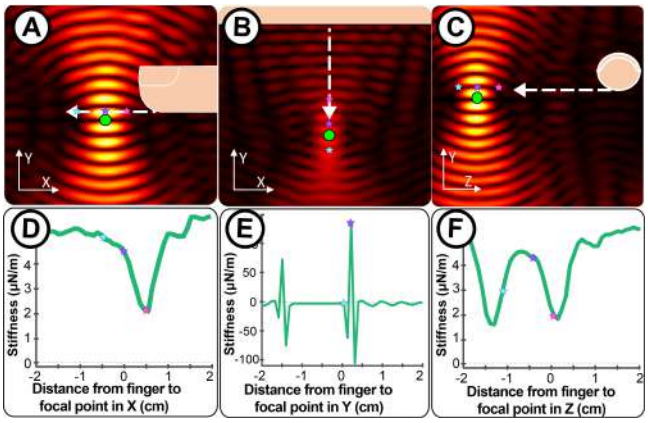

Figure 4: Trapping stiffness at a fixed point (green circle) as the finger slides in and out along different axis. a,b,c) amplitude fields and translation direction. Stiffness along: x-axis (d), y-axis (e), z-axis (f).

The following subsections describe the numerical FDTD simulations that informed the design of these 3 stages.

4.1 Analysis of Selection/Deselection

Section 3.2 demonstrated that *OTs* can trap particles, but TipTrap must also allow users to select (capture) and deselect (release) them. The challenge here is to identify strategies dealing with the transition from a particle levitating in a conventional trap, until it moves under the fingertip into the *OT*. More specifically, we look at how the trapping stiffness gets affected by different approaching directions of the user's finger and characterise their resilience to misalignment.

In order to identify optimum approaching directions of the fingertip towards a particle, we simulated a user's finger approaching a fixed levitated particle (inside a trap) from each direction (Figure 4). We looked at the trapping stiffness at that fixed particle as the finger slides in. This simulation can be used to characterise selection (i.e. finger sliding in, plots are read from right to left) or deselection (i.e. finger sliding out, plots are read from left to right). In general, the higher the stiffness, the more strongly a particle will be trapped. Positive values of stiffness indicate that the particle can remain trapped. Negative values, imply that particles cannot be trapped despite the power of the system and will be ejected.

The simulations shows that the particle can remained trapped as the finger slides in (select) or slides out (deselect) from the sides (X or Z). There is a decrease of the stiffness as the finger is entering or getting out (i.e., pink start when the finger is at $\sim$ 9 mm from the particle, in Figure 2.D and F), caused by a disturbance on the field but the traps remain functional and the stiffness soon increases and stabilizes as the fingertip passes this point (i.e., other stars).

Stiffness is always positive for selection/deselection from the sides (e.g. along axis X or Z) but not along the Y axis (Figure 2.E). In this case, the stiffness oscillates quickly with negative values every 4.2 mm ($\lambda/2$). Meaning that there are positions where trapping is not possible and the particle will be ejected if the finger approaches the particle from above or below.

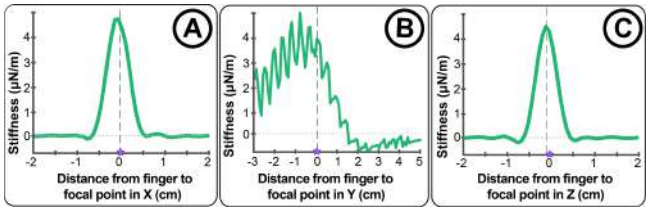

Figure 5: Trapping stiffness below the fingertip as the finger translates along: the x-axis (a), y-axis (b), and z-axis (c). The vertical dashed black line shows the optimum trapping finger position.

This analysis of the trapping stiffness shows that while selecting/deselecting a trapped particle is possible by approaching it from the sides (X or Z directions), it would not be possible to do it from the top (Y direction), as the acoustic reflections would cause the particle to be ejected (or to transition to secondary traps) when the negative values of the stiffness are observed in Figure 4.E. Thus, only horizontal approaching directions should be used for the selection and deselection stages in TipTrap.

4.2 Analysis of Manipulation

The previous subsection used simulations to identify the best way to select/deselect the particle, focusing on the transition from a levitation trap into an *OT* underneath the fingertip.

In this subsection, we focus on the effects that positional inaccuracies would have on the stiffness of the trap. These can be caused due to tracking errors or delays, but either case will result in a mismatch between the optimum location where the *OT* should be created (2.1 mm below the centre of the fingertip), and the location where the trap is actually being created. We hence look at these inaccuracies in terms of trap-to-OT distance mismatch, independently of its underlying cause.

4.2.1 Positional requirements. In order to analyse trapping quality during manipulation and in the presence of mismatches, we assume a particle already trapped below the user's fingertip. The user's fingertip is tracked continuously and a trap created under it, but with increasing positional errors (i.e., trap-to-OT distance mismatches).

Figure 5 simulates this situation, plotting the trapping stiffness at 2.1 mm below the fingertip as mismatch increases. Our results show that there is an operational range for each of the 3 axes, showing a positive stiffness below the finger tip even when the system is not exactly focusing at the optimum point. These results can be used to determine the positional error that TipTrap can tolerate.

For instance, trapping stiffness reduces to 50% for errors (mismatches) of 7 mm, 18mm and 7mm in X, Y and Z directions respectively. Taking the most conservative distances for each axis, this indicates that the tracking system should provide relatively high tracking accuracy along the horizontal direction, but this tolerance is more forgiving along the vertical direction.

4.2.2 Orientation Requirements. The previous simulations used a finger remaining perfectly horizontal, but this is not likely to happen during interaction. In fact, during preliminary tests we noticed that the angle of the finger changes naturally as the hand is

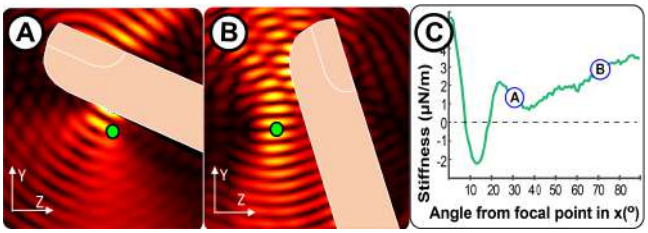

Figure 6: Trapping stiffness as the finger rotates from 0 to 90 degrees. a) Amplitude field at 30 degrees, b) Amplitude field at 70 degrees, c) Trapping stiffness at a fixed point as the finger rotates.

moved inside the levitator. Here, we consider that the orientation of the user's fingertip can vary during interaction and evaluate the effects on the trapping stiffness of such orientation change.

As the finger is almost cylindrical, rotations along its main axis (X) will not affect trapping significantly. Similarly, the employed levitation setup and traps are symmetric along the Y axis, and these rotations will not affect trapping either. As a result, we focus our analysis on the rotations around the Z axis (see Figures 6.A and B), as these cause dramatic changes in the acoustic field within the levitation space, either due to changes in reflection/scattering or as the top array stops being blocked by the finger and it starts to contribute again to the trap.

Figure 6.C shows the evolution of stiffness as the angle of the finger changes. From 0 to 10 degrees the stiffness indicates that the trap is functional but if the finger angle gets larger, the stiffness decreases and the particle will fall or get pushed to another position outside of the trap. At 20 degrees the trap becomes functional again, and beyond that point the trap improves since the finger is not blocking the field in a significant way. This indicates that, once the user has selected the particle, finger orientations can change ±10 degrees while retaining functional traps, allowing for some tolerance to involuntary rotations of the finger during manipulation.

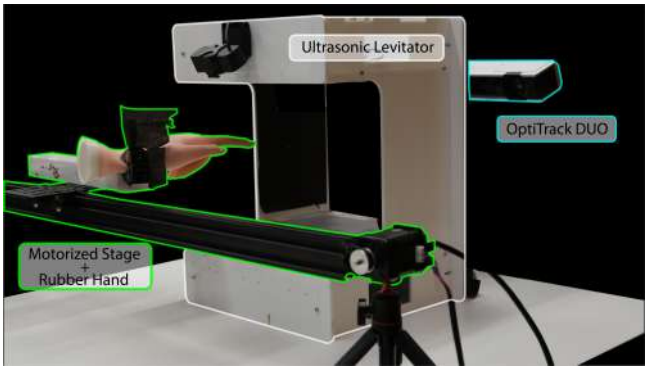

Figure 7: Overview of the components in our setup. We used two opposed phased arrays (PATs) separated by 24 cm, an OptiTrack Duo system to track the position of the fingertip in real-time, and a silicone hand attached to a motorized stage for emulating the user's interactions.

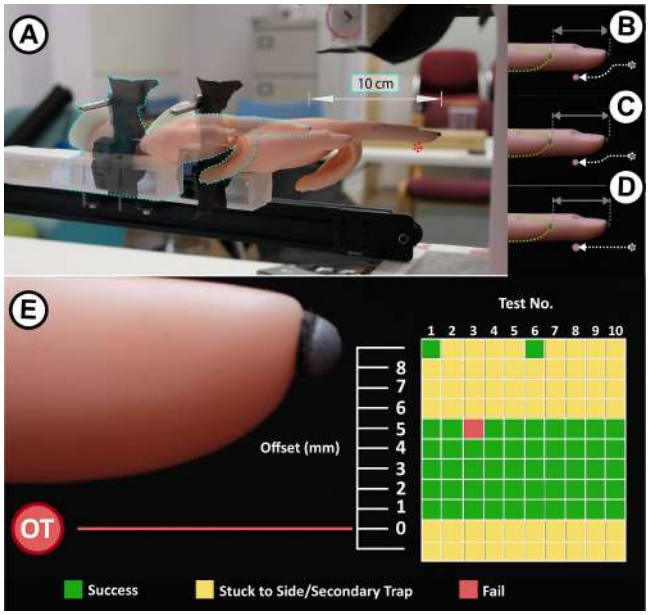

Figure 8: Characterising the *Selection* stage: a) Motorised setup with a linear stage and a silicone hand. b-d) height offsets (7, 4 and 0mm), and transition of particles to the *OT* (only the hand moved during the tests). e) Results from selection tests performed at different heights.

5 IMPLEMENTATION AND TECHNICAL CHARACTERIZATION

We implemented the TipTrap technique using the experimental setup in Figure 7. Our levitator uses two opposed arrays of 16×16 transducers as used in most display-based levitation systems [14, 28, 30], modified to operate at 20Vpp and higher update rates of 10kHz. The device generates multiple standing-wave traps at controlled positions using the method described in [40].

We used an OptiTrack Duo system and 2mm retro-reflective markers attached to the front of the fingertip. Traps are generated 15 mm behind and 8 mm below the position of the marker matching a distance of ~ 2 mm below the fingertip skin, thus creating a trap at the optimum position in relation to the finger. The use of a single marker did not allow us to retrieve orientation and the hands had to remain horizontal and perpendicular to the display during the tests. This is however a limitation of the tracking system used for our demonstration and not an implicit limitation of TipTrap.

Given the difficulties to conduct in-person tests with real users, we used a mechanical setup to mimic user interaction. More specifically, we used a commercially available silicone manicure practice hand attached to a NEMA17 belt-driven linear actuator with a 1.6A stepper motor (see 7). This setup was used to conduct controlled tests for characterising the performance of each step in TipTrap: Selection, Manipulation and Deselection.

5.1 Selection Tests

These tests measure the TipTrap *Selection* stage success rate at different height offsets between the levitated particle and the fingertip

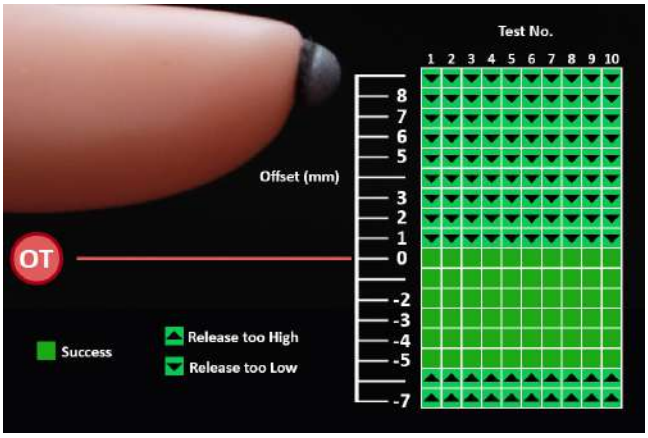

Figure 9: Characterising the *Deselect* stage. All tests showed successful results, with particles being trapped after *Deselect*. Particles will end up at the closest node of the trap, either at the primary trap location (i.e. green) or at secondary trap locations (i.e. arrows) above/below the trap.

(Y-direction). The silicone hand was moved in and out of the levitation area along the X-axis (see Figure 8.A). A particle was levitated in front of the fingertip, but at different vertical offsets (see Figure 8.B, C & D), where the 0 mm offset identifies the location of the *OT* (Figure 8.D). The silicone hand was then moved 4 cm along the X axis (horizontal), to position the particle in the *OT* under the fingertip.

We tested 10 different height offsets, from -8 mm to 2 mm from the reference of the optimum *OT* location. We conducted 10 tests for each height, and each test was considered successful only if the particle finished at the intended location of the *OT* (2.1 mm below the skin). Dropping or particles ending up at a secondary trap were considered as a failed test.

For offsets from -8 mm to -5 mm, the most usual outcome was a partial failure. That is, the particle did not transition into the *OT* or dropped, but instead it slid along the side of the fingertip finding a local trap to the side of the finger (see black region to the sides of the centre of the finger in Figure 2.C).

For offsets from -5 mm to 1 mm, transitions into the *OT* were highly reliable (one failure out of 50 attempts). This would be the ideal operational range for the *match height* stage of our technique (see Figure 3.B) and leads to our recommendation to match heights slightly above the final location of the *OT*.

For larger offsets, the particle engages with the high pressure region between the primary and secondary traps, causing the particle to move into the secondary trap (i.e. at 6.3 mm, instead of 2.1 mm, below the fingertip). This is a comparatively minor issue, as its trapping intensity is very similar to that of the primary trap, providing similar manipulation capabilities. It is not possible to move the particle upwards into the primary *OT* trap, but this adjustment would be easy to implement by refocusing the trap if particle tracking is available, using a trapping correction technique such as the one described in [3].

5.2 Deselect Tests

These tests check the performance of our *Deselection* stage, using a setup similar to that in Figure 8.A. We first placed the particle into the primary *OT* underneath the silicone fingertip, and simulated the effects of the *Deselect* stage with various height mismatch errors. More specifically, the acoustic trap remained at a fixed point while the silicone hand was moved out (4 cm backwards). The mismatch error is the distance between that fixed trap position and the location where the *OT* appears (2.1 mm below the skin). Releasing at each height was repeated 10 times. We used our tracking system to check the final location of the particle and tests were considered successful only if the particle ended up at the primary levitation trap. Any other cases such as the particle ending up in secondary traps above/below or dropping were considered a failure.

Results in Figure 9 show a much more reliable behaviour than the selection tests, with not a single particle being dropped across all the 170 tests. The optimum operational range is identified between 0-6 mm offsets. In this cases, the particle will be able to overcome the height mismatch between the *OT* and the levitation trap, ending up at the primary trap location. Results outside this 0-6 mm range simply show that the particle will transition to the closest trap location which, in this cases, will be a secondary trap 4.2 mm above or below the primary node.

5.3 Manipulation Tests

These tests were conducted to characterise our *Manipulation* stage, by moving the particle across the levitation stage with variable amounts of tracking error and increasing speeds, as shown in Figure 10.A. More specifically, a particle was placed at the *OT* and the hand moved 10 cm horizontally. The location of the trap was retrieved from our tracking system and a variable offset applied along the vertical (Y) axis.

The height offsets ranged from -5mm to 5mm, as offsets beyond ±4.3mm would create a secondary trap in one of the positions already covered by our ± 5mm range. The hand would then move back and forth along the X-axis, with the trap being refocused under the fingertip position (with the required height offset), as detected by our tracking system.

During this motion, speed increased linearly using the maximum acceleration allowed by our setup (10 cm/s^2), until the maximum target speed was reached. Such speed was maintained during the middle of the task and linearly decelerated towards the end of the task. The maximum speeds for such speed profiles started at 1 cm/s and was increased by 1 cm/s in each successive iteration, until the maximum speed of 10 cm/s was reached.

The tracking system was used to determine the location of the trap, but no additional techniques were used to counteract delays in processing or noise. This was done to avoid over-fitting to our known velocity profiles, and to better reflect a real tracking system. The test was deemed successful if the particle remained within the primary *OT* at the end of the test and each test was repeated 10 times.

These tests show that tracking errors along the Y (vertical) axis can be large during the *Manipulation* stage and the technique will still work. The majority of the tests yielded functional results, as the

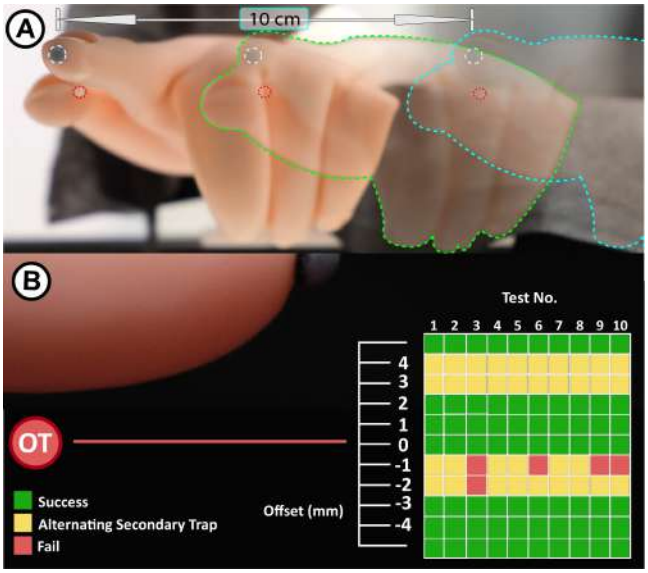

Figure 10: Characterizing the Manipulation stage: a) Range of motion used by our setup for this test. b) Results from manipulations tests performed at various particle height offsets and manipulation speeds.

particle would stay trapped almost regardless of the height offset and speed.

Results are even more positive when the nodes of the *OT* and the levitation trap are aligned. Given the separation of 4.3 mm between nodes, this happens for height offsets between 0 to 2 mm and -3 to -5 mm. In these cases, a particle escaping the *OT* (e.g., misalignment causes ultrasound to miss and not reflect off the finger) could still safely transition into the levitation trap, as the nodes in this trap are aligned to those in the *OT*. Within these ranges, the effect of the offset was not noticeable and all tests were successful.

However, for other height offsets the nodes of the *OT* and levitation trap would not align (e.g., for a height of -2mm each node of the *OT* actually aligns with an anti-node of the levitation trap, if ultrasound missed the fingertip). In these cases, the particle would shift upwards/downwards into the levitation trap, searching for these misaligned nodes. This could cause the particle to slide from one side of the finger to another depending on the direction of the movement, or to fail completely in some cases between -1 and -2 mm offsets.

6 INTERACTION EXAMPLES

TipTrap is a generic selection and manipulation technique for levitation-based displays, that can be applied to interact with games, visualizations, notifications and other levitation applications demonstrated to date. However, as a unique feature, it allows users to approach such tasks using co-located direct interaction, instead of interacting at a distance.

This section explores the use of TipTrap for direct co-located manipulation of levitated content in an application-agnostic manner (see Figure 11). More specifically, we focus on the types of levitated content identified by Fender et al. [11]: i) independent particles; ii) levitated props; and iii) POV content, deriving factors to consider when using TipTrap to manipulate each of these contents. Our examples were implemented using the thumb gestures: flexion to select, extension to deselect. Other gestures or modalities (e.g. voice commands) could be used instead.

6.1 Manipulating independent particles

We created a game-like example to demonstrate co-located interaction with independent particles. The application shows different 3D shapes made of independent particles, one at a time (i.e., squares, triangles, pentagons, pyramids, and cubes). The user must try to remember the original location of each particle and move it there after the system arranges them randomly. Each trial of this game has 3 stages shown in Figure 11.A:

- *Exposure stage*: the target geometry is shown for 3 seconds, for users to memorise it.
- *Disassembly stage*: the 3D shape is disassembled and all the particles are automatically moved to the right of the rendering volume.
- *Reconstruction stage*: The user must use TipTrap technique to select, move and release each of the primitives arranged on the side to reconstruct the original geometry.

This example illustrates the simplest type of manipulation, with TipTrap being used to manipulate multiple particles individually. It must be noted that the reliability of the technique is influenced by the number of particles used, as trapping stiffness decreases as more particles are levitated simultaneously [28].

Minimum distances between particles must be considered to disambiguate the specific particle being selected, as well as to allow enough space for the users' hands and fingers. Collision avoidance algorithms should also be considered [43].

6.2 Manipulating levitated props

We created a simple application exploring the control of a *LeviProp* [31] used as a levitated mini-screen. Figures 11.B, C and 1.D demonstrate *LeviProps* made of 3 and 4 particles respectively. In either case, the particles in the prop can be used as manipulation gizmos. Although only translations of the prop as a whole are shown, other implementations could assign specific purposes to each particle such as scaling or rotation. The use of bi-manual interaction (see video figure) can provide additional interaction possibilities like supporting content rotations around arbitrary axes.

The use of co-located direct manipulations of the *LeviProp* must be considered when designing the prop itself. The ultrasound reflected off the fingertip will create the *OT* required by TipTrap to control that specific particle. However, this same reflected ultrasound can interfere with other particles in the *LeviProp*, particularly for particles in close proximity or strictly above/below the target particle (i.e. Figure 2.B shows significant effects for particles placed 3 cm below the finger). This could either be considered when designing the *LeviProp*, or avoided by giving additional vertical spacing.

Apart from manipulating the particles of the prop itself, external individual particles away from the *LeviProp* can also be used as controllers to adjust various aspects of the levitated content and to trigger specific animations or modes), or simply for convenience by

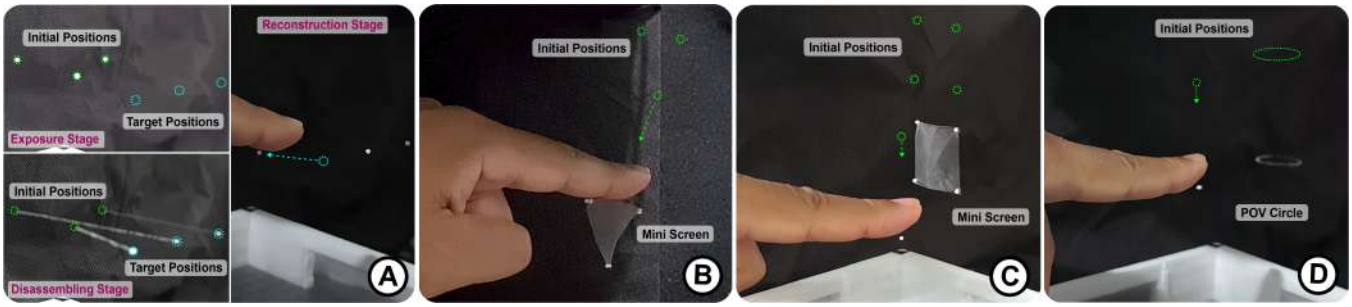

Figure 11: Four TipTrap application examples: a) matching 3D constellations, b, c) levitated props arrangement (direct and indirect anchor points) and d) fast-moving particle (PoV content) manipulation.

avoiding fingers occluding the image projected on the prop when moving it, such as in the remote prop manipulator in Figure 11.C).

6.3 PoV content

Figure 11.D shows an external individual particle 4 cm in front of a simple POV shape (i.e. horizontal circle, 3cm diameter). Users can use the external particle to control the location of the POV content.

Co-located, direct control of the POV shape was unreliable with the basic TipTrap technique described in this paper. When the tracer particle approached the fingertip at the matched height, the particle would get pushed down into a secondary trap (i.e., 6.3 mm below the fingertip), distorting the shape while going under the finger, or even getting ejected due to its large speed (> 5m/s). This was the case for a flat horizontal shape such as the one in our example, even if the POV shape matched the height of the *OT* (i.e. < 2 mm under the user's fingertip). As such, TipTrap direct manipulation of POV content will need to consider such finger-POV path interactions and requires further investigation.

7 DISCUSSION

This paper described and proposed the TipTrap technique, providing an analytical and experimental exploration as well as demonstrating novel interaction possibilities by allowing the co-located direct manipulation of levitated content. However, other aspects relevant to the technique will require further investigation.

First of all, the whole application space where the technique can be applied cannot be addressed within the scope of this paper. Our characterization indicates that the introduction of the technique does not reduce the strength of the traps (e.g., see force comparison of OTs vs traditional traps in Figure 2) and, as such, the application space should be very similar to systems not using TipTrap.

However, even if traps are physically similar, the differences in co-located vs at-a-distance interaction could introduce their own differences such as more jitter in the hand since it cannot be fully rested on a table. Promising lines of future research for TipTrap should address comparative evaluations with related indirect techniques, such as Point&Shake [13] (i.e., for selection) or LeviCursor [3] (i.e. for manipulation). Such explorations should also consider the use of a variable number of levitated particles, comparisons of single vs bi-manual TipTrap interaction, or even studies in the context of specific applications.

We used flexion and unbending of the thumb as gestures to trigger selection or deselection. This was just done for illustrative purposes and, other gestures could be used instead. Elicitation studies would then be required to identify the most effective and intuitive gestures/commands to select, manipulate and deselect levitated content.

Another aspect to consider for a complete technique is the inclusion of feedback (e.g., to confirm selection/release). Ultrasound tactile feedback is perceivable by modulating the amplitude of the trap under the fingertip at a frequency of 200Hz. This is useful only if a small number of particles are used since perceived intensity will be reduced as the number of particles increases [40]. Thus, visual or auditive feedback can provide a more feasible and general solution.

Other future extensions are related to the type of content manipulated, as explained in Section 6. These include the introduction of collision avoidance techniques considering the hand volume, the extension of LeviProp designs to account for finger reflections, or adjustments to PoV rendering to allow for direct manipulation.

We limited our exploration to *OTs* created below the fingertip. However, the employed top-bottom setup can also create *OTs* above the fingertip by reflecting the ultrasound from the top board and occluding that from the bottom one. This would allow the particle to be placed at the most convenient location to facilitate visibility (e.g., place it above the fingertip when interaction is below eye level).

We also limited our exploration to finger-like structures, but *OTs* can be applied to other shapes or tools such as a stylus, opening scenarios for augmented reality and interaction through tokens.

Finally, we used an OptiTrack for the tracking of the hand during our tests. We tried markerless solutions such as Leap motion but caused detection issues given the transducers in the background or close proximity of the hands. We consider these tracking issues beyond the scope of the paper, but interested practitioners should be aware of such challenges.

8 CONCLUSION

We have presented TipTrap, a novel manipulation technique for acoustic levitation displays which exploits the acoustically reflective properties of the user's fingertip to enable direct co-located manipulation of levitated content. We characterized the trapping stiffness of *Opportunistic Traps*, showing how the quality of such traps is very similar to that of a conventional levitation trap. We

then provided an analytical exploration using FDTD simulations to identify feasible strategies to select, manipulate and deselect levitated particles, paying particular attention to the transitions of the particles between conventional levitation traps and opportunistic traps below the fingertips, as well as their tolerance towards position and orientation errors. We then implemented the TipTrap technique and provided a technical characterization of its performance, using a mechanical setup and a silicone hand to demonstrate how the technique can provide robust selection, manipulation and deselection. We finally demonstrated example applications, showcasing the potential of this technique to manipulate different types of levitated content. To our knowledge, this is the first instance of a direct co-located interaction technique for levitated content, and one which we believe that will open new opportunities and applications within these emergent interfaces.

ACKNOWLEDGMENTS

This research was funded by the EU Horizon 2020 research and innovation programme under grant agreement No 101017746 TOUCHLESS, the AHRC UK-China Research-Industry Creative Partnerships (AH/T01136X/2) and EPSRC and Ultraleap Prosperity Fund (EP/V037846/1).

REFERENCES

[1] Andrew Allen and Nikunj Raghuvanshi. 2015. Aerophones in flatland: Interactive wave simulation of wind instruments. *ACM Transactions on Graphics (TOG)* 34, 4 (2015), 1–11.

[2] Marco AB Andrade, Thales SA Camargo, and Asier Marzo. 2018. Automatic contactless injection, transportation, merging, and ejection of droplets with a multifocal point acoustic levitator. *Review of Scientific Instruments* 89, 12 (2018), 125105.

[3] Myroslav Bachynskyi, Viktorija Paneva, and Jörg Müller. 2018. LeviCursor: Dexterous Interaction with a Levitating Object. In *Proceedings of the 2018 ACM International Conference on Interactive Surfaces and Spaces*. 253–262.

[4] R. Balakrishnan, G.W. Fitzmaurice, and G. Kurtenbach. 2001. User interfaces for volumetric displays. *Computer* 34, 3 (2001), 37–45. https://doi.org/10.1109/2.910892

[5] Peter C Barnum, Srinivasa G Narasimhan, and Takeo Kanade. 2010. A multi-layered display with water drops. In *ACM SIGGRAPH 2010 papers*. 1–7.

[6] Johann Berthelot and Nicolas Bonod. 2019. Free-space micro-graphics with electrically driven levitated light scatterers. *Optics letters* 44, 6 (2019), 1476–1479.

[7] Richard W Bowen, Jordan Pola, and Leonard Matin. 1974. Visual persistence: Effects of flash luminance, duration and energy. *Vision Research* 14, 4 (1974), 295–303.

[8] Doug A. Bowman, Donald B. Johnson, and Larry F. Hodges. 1999. Testbed Evaluation of Virtual Environment Interaction Techniques. In *Proceedings of the ACM Symposium on Virtual Reality Software and Technology* (London, United Kingdom) *(VRST '99)*. Association for Computing Machinery, New York, NY, USA, 26–33. https://doi.org/10.1145/323663.323667

[9] Shin-ichiro Eitoku, Kunihiro Nishimura, Tomohiro Tanikawa, and Michitaka Hirose. 2009. Study on design of controllable particle display using water drops suitable for light environment. In *Proceedings of the 16th ACM Symposium on Virtual Reality Software and Technology*. 23–26.

[10] Iñigo Ezcurdia, Adriana Arregui, Oscar Ardaiz, Amalia Ortiz, and Asier Marzo. 2020. Content Adaptation and Depth Perception in an Affordable Multi-View Display. *Applied Sciences* 10, 20 (2020), 7357.

[11] Andreas Rene Fender, Diego Martinez Plasencia, and Sriram Subramanian. 2021. *ArticuLev: An Integrated Self-Assembly Pipeline for Articulated Multi-Bead Levitation Primitives*. Association for Computing Machinery, New York, NY, USA. https://doi.org/10.1145/3411764.3445342

[12] Euan Freeman, Asier Marzo, Praxitelis B. Kourtelos, Julie R. Williamson, and Stephen Brewster. 2019. Enhancing Physical Objects with Actuated Levitating Particles. In *Proceedings of the 8th ACM International Symposium on Pervasive Displays* (Palermo, Italy) *(PerDis '19)*. Association for Computing Machinery, New York, NY, USA, Article 2, 7 pages. https://doi.org/10.1145/3321335.3324939

[13] Euan Freeman, Julie Williamson, Sriram Subramanian, and Stephen Brewster. 2018. Point-and-shake: selecting from levitating object displays. In *Proceedings of the 2018 CHI Conference on Human Factors in Computing Systems*. 1–10.

[14] Tatsuki Fushimi, Asier Marzo, Bruce W Drinkwater, and Thomas L Hill. 2019. Acoustophoretic volumetric displays using a fast-moving levitated particle. *Applied Physics Letters* 115, 6 (2019), 064101.

[15] Lev Petrovich Gor'kov. 1961. Forces acting on a small particle in an acoustic field within an ideal fluid. In *Doklady Akademii Nauk*, Vol. 140. Russian Academy of Sciences, 88–91.

[16] Martin Hachet, Benoit Bossavit, Aurélie Cohé, and Jean-Baptiste de la Rivière. 2011. Toucheo: multitouch and stereo combined in a seamless workspace. In *Proceedings of the 24th annual ACM symposium on User interface software and technology*. 587–592.

[17] Otmar Hilliges, David Kim, Shahram Izadi, Malte Weiss, and Andrew Wilson. 2012. HoloDesk: direct 3d interactions with a situated see-through display. In *Proceedings of the SIGCHI Conference on Human Factors in Computing Systems*. 2421–2430.

[18] Ryuji Hirayama, Diego Martinez Plasencia, Nobuyuki Masuda, and Sriram Subramanian. 2019. A volumetric display for visual, tactile and audio presentation using acoustic trapping. *Nature* 575, 7782 (2019), 320–323.

[19] Edwin L Hutchins, James D Hollan, and Donald A Norman. 1985. Direct manipulation interfaces. *Human–computer interaction* 1, 4 (1985), 311–338.

[20] Andrew Jones, Ian McDowall, Hideshi Yamada, Mark Bolas, and Paul Debevec. 2007. Rendering for an interactive 360 light field display. In *ACM SIGGRAPH 2007 papers*. 40–es.

[21] Abhijit Karnik, Diego Martinez Plasencia, Walterio Mayol-Cuevas, and Sriram Subramanian. 2012. PiVOT: personalized view-overlays for tabletops. In *Proceedings of the 25th annual ACM symposium on User interface software and technology*. 271–280.

[22] Jinha Lee, Alex Olwal, Hiroshi Ishii, and Cati Boulanger. 2013. SpaceTop: integrating 2D and spatial 3D interactions in a see-through desktop environment. In *Proceedings of the SIGCHI Conference on Human Factors in Computing Systems*. 189–192.

[23] Jinha Lee, Rehmi Post, and Hiroshi Ishii. 2011. ZeroN: Mid-Air Tangible Interaction Enabled by Computer Controlled Magnetic Levitation. In *Proceedings of the 24th Annual ACM Symposium on User Interface Software and Technology* (Santa Barbara, California, USA) *(UIST '11)*. Association for Computing Machinery, New York, NY, USA, 327–336. https://doi.org/10.1145/2047196.2047239

[24] Diego Martinez Plasencia, Florent Berthaut, Abhijit Karnik, and Sriram Subramanian. 2014. Through the combining glass. In *Proceedings of the 27th annual ACM symposium on User interface software and technology*. 341–350.

[25] Diego Martinez Plasencia, Edward Joyce, and Sriram Subramanian. 2014. MisTable: Reach-through Personal Screens for Tabletops. In *Proceedings of the SIGCHI Conference on Human Factors in Computing Systems* (Toronto, Ontario, Canada) *(CHI '14)*. Association for Computing Machinery, New York, NY, USA, 3493–3502. https://doi.org/10.1145/2556288.2557325

[26] Asier Marzo. 2016. GauntLev: A wearable to manipulate free-floating objects. In *Proceedings of the 2016 CHI Conference on Human Factors in Computing Systems*. 3277–3281.

[27] Asier Marzo, Tom Corkett, and Bruce W Drinkwater. 2017. Ultraino: An open phased-array system for narrowband airborne ultrasound transmission. *IEEE transactions on ultrasonics, ferroelectrics, and frequency control* 65, 1 (2017), 102–111.

[28] Asier Marzo and Bruce W Drinkwater. 2019. Holographic acoustic tweezers. *Proceedings of the National Academy of Sciences* 116, 1 (2019), 84–89.

[29] Asier Marzo, Sue Ann Seah, Bruce W Drinkwater, Deepak Ranjan Sahoo, Benjamin Long, and Sriram Subramanian. 2015. Holographic acoustic elements for manipulation of levitated objects. *Nature communications* 6, 1 (2015), 1–7.

[30] Rafael Morales, Iñigo Ezcurdia, Josu Irisarri, Marco A. B. Andrade, and Asier Marzo. 2021. Generating Airborne Ultrasonic Amplitude Patterns Using an Open Hardware Phased Array. *Applied Sciences* 11, 7 (2021). https://doi.org/10.3390/app11072981

[31] Rafael Morales, Asier Marzo, Sriram Subramanian, and Diego Martínez. 2019. LeviProps: Animating levitated optimized fabric structures using holographic acoustic tweezers. In *Proceedings of the 32nd Annual ACM Symposium on User Interface Software and Technology*. 651–661.

[32] Rafael Morales González, Euan Freeman, and Orestis Georgiou. 2020. Levi-Loop: A Mid-Air Gesture Controlled Levitating Particle Game. In *Extended Abstracts of the 2020 CHI Conference on Human Factors in Computing Systems* (Honolulu, HI, USA) *(CHI EA '20)*. Association for Computing Machinery, New York, NY, USA, 1–4. https://doi.org/10.1145/3334480.3383152

[33] Mohd Adili Norasikin, Diego Martinez Plasencia, Spyros Polychronopoulos, Gianluca Memoli, Yutaka Tokuda, and Sriram Subramanian. 2018. SoundBender: dynamic acoustic control behind obstacles. In *Proceedings of the 31st Annual ACM Symposium on User Interface Software and Technology*. 247–259.

[34] Yoichi Ochiai, Takayuki Hoshi, and Jun Rekimoto. 2014. Pixie dust: graphics generated by levitated and animated objects in computational acoustic-potential field. *ACM Transactions on Graphics (TOG)* 33, 4 (2014), 1–13.

[35] Themis Omirou, Asier Marzo, Sue Ann Seah, and Sriram Subramanian. 2015. LeviPath: Modular acoustic levitation for 3D path visualisations. In *Proceedings of the 33rd Annual ACM Conference on Human Factors in Computing Systems*.

309–312.

[36] T. Omirou, A. M. Perez, S. Subramanian, and A. Roudaut. 2016. Floating charts: Data plotting using free-floating acoustically levitated representations. In *2016 IEEE Symposium on 3D User Interfaces (3DUI)*. 187–190. https://doi.org/10.1109/3DUI.2016.7460051

[37] Viktorija Paneva, Myroslav Bachynskyi, and Jörg Müller. 2020. *Levitation Simulator: Prototyping Ultrasonic Levitation Interfaces in Virtual Reality*. Association for Computing Machinery, New York, NY, USA, 1–12. https://doi.org/10.1145/3313831.3376409

[38] Viktorija Paneva, Arthur Fleig, Diego Martínez Plasencia, Timm Faulwasser, and Jörg Müller. 2022. OptiTrap: Optimal Trap Trajectories for Acoustic Levitation Displays. *ACM Trans. Graph.* (feb 2022). https://doi.org/10.1145/3517746 Just Accepted.

[39] Kenneth Perlin et al. 2006. Volumetric display with dust as the participating medium. US Patent 6,997,558.

[40] Diego Martinez Plasencia, Ryuji Hirayama, Roberto Montano-Murillo, and Sriram Subramanian. 2020. GS-PAT: high-speed multi-point sound-fields for phased arrays of transducers. *ACM Transactions on Graphics (TOG)* 39, 4 (2020), 138–1.

[41] Timothy Poston and Luis Serra. 1994. The virtual workbench: Dextrous VR. In *Virtual reality software and technology*. World Scientific, 111–121.

[42] Ismo Rakkolainen. 2008. Mid-air displays enabling novel user interfaces. In *Proceedings of the 1st ACM international workshop on Semantic ambient media experiences*. 25–30.

[43] Maxime Reynal, Euan Freeman, and Stephen Brewster. 2020. Avoiding Collisions When Interacting with Levitating Particle Displays. In *Extended Abstracts of the 2020 CHI Conference on Human Factors in Computing Systems* (Honolulu, HI, USA) *(CHI EA '20)*. Association for Computing Machinery, New York, NY, USA, 1–7. https://doi.org/10.1145/3334480.3382965

[44] Deepak Ranjan Sahoo, Diego Martinez Plasencia, and Sriram Subramanian. 2015. Control of Non-Solid Diffusers by Electrostatic Charging. In *Proceedings of the 33rd Annual ACM Conference on Human Factors in Computing Systems* (Seoul, Republic of Korea) *(CHI '15)*. Association for Computing Machinery, New York, NY, USA, 11–14. https://doi.org/10.1145/2702123.2702363

[45] Hideo Saito, Hidei Kimura, Satoru Shimada, Takeshi Naemura, Jun Kayahara, Songkran Jarusirisawad, Vincent Nozick, Hiroyo Ishikawa, Toshiyuki Murakami, Jun Aoki, et al. 2008. Laser-plasma scanning 3D display for putting digital contents in free space. In *Stereoscopic Displays and Applications XIX*, Vol. 6803. International Society for Optics and Photonics, 680309.

[46] Lina Sawalha, Monte P Tull, Matthew B Gately, James J Sluss, Mark Yeary, and Ronald D Barnes. 2012. A large 3D swept-volume video display. *Journal of Display Technology* 8, 5 (2012), 256–268.

[47] Takashi Shibata, Joohwan Kim, David M Hoffman, and Martin S Banks. 2011. The zone of comfort: Predicting visual discomfort with stereo displays. *Journal of vision* 11, 8 (2011), 11–11.

[48] DE Smalley, E Nygaard, K Squire, J Van Wagoner, J Rasmussen, S Gneiting, K Qaderi, J Goodsell, W Rogers, M Lindsey, et al. 2018. A photophoretic-trap volumetric display. *Nature* 553, 7689 (2018), 486–490.

[49] Daniel Smalley, Ting-Chung Poon, Hongyue Gao, Joshua Kvavle, and Kamran Qaderi. 2018. Volumetric displays: turning 3-D inside-out. *Optics and Photonics News* 29, 6 (2018), 26–33.

[50] Alan Sullivan. 2004. DepthCube solid-state 3D volumetric display. In *Stereoscopic displays and virtual reality systems XI*, Vol. 5291. International Society for Optics and Photonics, 279–284.

[51] Yutaka Tokuda, Mohd Adili Norasikin, Sriram Subramanian, and Diego Martinez Plasencia. 2017. MistForm: Adaptive Shape Changing Fog Screens. In *Proceedings of the 2017 CHI Conference on Human Factors in Computing Systems* (Denver, Colorado, USA) *(CHI '17)*. Association for Computing Machinery, New York, NY, USA, 4383–4395. https://doi.org/10.1145/3025453.3025608